Improved Quality of Pediatric ^{123}I-MIBG Images with Medium-Energy Collimators

Erin R. Snay, CNMT, S. Ted Treves, and Frederic H. Fahey

Division of Nuclear Medicine and Molecular Imaging, Children's Hospital Boston, Boston, Massachusetts

Our objective was to optimize the quality of ^{123}I-metaiodobenzylguanidine (MIBG) scans by using a medium-energy collimator to reduce high-energy-photon septal penetration. **Methods:** In addition to the 159-keV γ-ray, ^{123}I has a small abundance of energies above 400 keV that can compromise the image quality of MIBG studies because of septal penetration. Using a low-energy ultrahigh-resolution collimator (LEUHR), a low-energy high-resolution collimator (LEHR), and a medium-energy collimator, we obtained and compared SPECT and planar images of a SPECT phantom filled with ^{123}I. These studies were acquired at a count level comparable to clinical MIBG images, 24,000 counts per view for SPECT and 300,000 counts for planar imaging. Also, we evaluated the sensitivity of the 3 collimators at 0 and 10 cm using the National Electrical Manufacturers Association protocol. **Results:** The image quality for both SPECT and planar ^{123}I images using the medium-energy collimator was determined to be substantially better than that using the LEUHR or LEHR collimator. The septa of the medium-energy collimator are thicker than those of the low-energy collimators (1.14 vs. 0.13–0.16 mm), leading to a significant reduction in septal penetration of the high-energy γ-rays and a marked improvement in image quality. The sensitivity for the medium-energy collimator did not change with distance (8.00 cpm/kBq), as opposed to the LEUHR collimator (6.59 and 5.51 cpm/kBq for 0 and 10 cm, respectively) and the LEHR collimator (14.32 and 12.30 cpm/kBq for 0 and 10 cm, respectively). This variation in sensitivity for the LEUHR collimator is again due to the presence of high-energy photons. **Conclusion:** Use of a medium-energy collimator substantially improves the quality of both planar and SPECT ^{123}I images. We recommend that a medium-energy collimator routinely be used for ^{123}I-MIBG imaging.

Key Words: SPECT; ^{123}I-MIBG; pediatric; planar scintigraphy

J Nucl Med Technol 2011; 39:100–104
DOI: 10.2967/jnmt.110.080309

In the past several years, many radiopharmaceuticals, including metaiodobenzylguanidine (MIBG), that were formerly labeled with ^{131}I are now labeled with ^{123}I because it has better dosimetric and imaging properties (*1–3*). ^{123}I decays by electron capture, with a 13.2-h half-life. The primary γ-ray of its daughter, ^{123}Te, has an energy of 159 keV. In addition to the 159-keV γ-ray (83.3% abundance), several other γ-rays of higher energy and low abundance are also emitted as a result of the decay of ^{123}I. Several of these emissions are summarized in Table 1 (*4*). γ-rays with energies greater than 400 keV are emitted 2.73% of the time, and γ-rays with energies greater than 600 keV are emitted 0.23% of the time. The average energy of the higher-energy γ-rays is 507 keV. Although these high-energy γ-rays are in low abundance, the low-energy collimators traditionally used for ^{123}I-MIBG imaging are not effective in stopping them. The result—substantial septal penetration (i.e., the fraction of γ-rays that cross the septa separating the collimator holes)—can, in turn, lead to a loss of contrast and image quality.

Figure 1 shows a cross section of a parallel-hole collimator (not drawn to scale). The maximum septal penetration will occur when the γ-ray barely misses the top of 1 septum, traverses the adjacent septum, and then barely misses the bottom of the third septum. Consider the characteristics of the low-energy ultrahigh-resolution collimator (LEUHR, traditionally used in our clinic for ^{123}I-MIBG imaging) and the medium-energy collimator used with the e.cam dual-detector SPECT γ-camera (Siemens Medical Solutions) as presented in Table 2. Also listed in this table are the maximum septal penetrations for 159-, 300-, and 500-keV photons. Although the septal thickness of 0.13 mm for the LEUHR is adequate for limiting septal penetration for 159 keV (<2.0%), it is not as effective at stopping higher-energy photons, leading to maximum penetration values of 42% and 71% for 300 and 500 keV, respectively. A substantial fraction of these photons will undergo Compton scatter in the γ-camera crystal, leading to detection of a large number of these higher-energy photons in the 159-keV energy window. In fact, it has been shown that almost half the photons detected in the 159-keV energy window using low-energy collimation resulted from these higher-energy photons (*5*).

Medium-energy collimators have thicker septa than low-energy collimators, leading to less septal penetration. As indicated in Table 2, the septal thickness for the medium-energy collimator is almost 10 times that of the LEUHR

Received Jun. 17, 2010; revision accepted Dec. 17, 2010.
For correspondence or reprints contact: Erin R. Snay, CNMT, Division of Nuclear Medicine and Molecular Imaging, Children's Hospital Boston, 300 Longwood Ave., Boston, MA 02115.
E-mail: erin.snay@childrens.harvard.edu

TABLE 1
γ-Ray Emissions from ^{123}I (*4*)

Energy (keV)	γ-rays per decay
159	0.828
248	0.0007
281	0.0008
346	0.0013
440	0.0043
505	0.0031
529	0.0138
539	0.0038
625	0.0008
688	0.0003
736	0.0006
784	0.0006

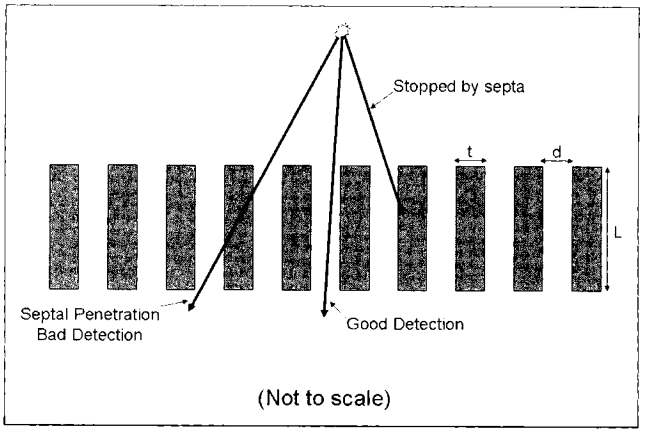

FIGURE 1. This figure shows 3 γ-rays being emitted from a point source at top of figure. γ-ray labeled "Good Detection" passes right through collimator hole and will be properly localized directly below point source. γ-ray labeled "Stopped by septa" hits septa and interacts, presumably by photoelectric effect, in septum and thus does not reach scintillation crystal. However, γ-ray labeled "Septal Penetration Bad Detection" passes through septum, reaching scintillation crystal at wrong location, not directly below point source. Probability for septal penetration depends on energy of incident γ-ray and thickness of septum. d = hole diameter; L = hole length; t = thickness of interhole septa.

collimator (1.14 and 0.13 mm, respectively), leading to a substantial reduction in maximum septal penetration, particularly for photons with energies between 300 and 500 keV. Investigators have recommended the use of medium-energy collimators for cardiovascular and neurologic imaging with ^{123}I (*6,7*). One investigator has recommended using medium-energy collimators for cardiovascular imaging but using a low-energy high-resolution (LEHR) collimator for neurologic imaging (*8*). However, to our knowledge, the utility of medium-energy collimators for pediatric tumor imaging has not previously been published. Therefore, we sought to determine whether the use of medium-energy collimators may, in fact, improve image quality for both planar nuclear imaging and SPECT and thereby be appropriate for ^{123}I-MIBG imaging in children. This investigation involved a phantom study and a preliminary clinical evaluation.

MATERIALS AND METHODS

Using the protocol specified by the National Electrical Manufacturers Association (report NU1) (*9*), we evaluated the sensitivity of ^{123}I on LEUHR, LEHR, and medium-energy collimators on a dual-detector e.cam γ-camera. A culture flask was filled with 13.9 MBq (0.377 mCi) of ^{123}I and counted for 1 min at 0 and 10 cm from the collimator surface.

A Jaszczak deluxe tomographic phantom (Data Spectrum) was filled with 163 MBq (4.4 mCi) of ^{123}I. The hot-rod insert was used for these measurements because ^{123}I-MIBG clinical studies represent a hot-spot detection task. This phantom was used for evaluating both planar imaging and SPECT. For planar imaging, the Jaszczak phantom was placed on the collimator face and imaged for 300,000 counts with the LEUHR, LEHR, and medium-energy collimators. We chose 300,000 counts because this is the number of counts we routinely acquire for planar ^{123}I-MIBG studies. For SPECT, each projection was acquired for 24,000 counts per view. Again, the number of counts acquired per view was similar to a clinical ^{123}I-MIBG SPECT study performed in our clinic. The study was acquired with 120 views per detector over 360°. The SPECT data were reconstructed

TABLE 2
Characteristics of 3 Collimators

Parameter	LEUHR	LEHR	Medium-energy
Septal thickness (mm)	0.13	0.16	1.14
Hole diameter (mm)	1.16	1.11	2.94
Hole length (mm)	35.8	24.05	40.64
Extrinsic sensitivity (cpm/kBq)*	2.70	5.46	8.38
Spatial resolution (mm)	4.6	6.4	10.8
Septal penetration at 159 keV	2.0%	3.5%	0.0%
Septal penetration at 300 keV	42%	48%	4.90%
Septal penetration at 500 keV	71%	75%	30%

*At 140 keV.

using filtered backprojection with a third-order Butterworth having a cutoff frequency of 0.4 cycles per Nyquist frequency.

In addition to the phantom study, 2 patient studies (1 imaged with ^{123}I-MIBG and 1 with ^{123}I-NaI to search for thyroid cancer metastases) were compared using both collimators. In the spring of 2005, our clinic amended its ^{123}I imaging protocols to use a medium-energy collimator. In the 2 clinical cases presented, the patients were initially imaged using the LEUHR collimator, and when they returned for routine follow-up several months later, they were imaged with the medium-energy collimator.

RESULTS

The results of the sensitivity measurements are shown in Table 3. The manufacturer's sensitivity specifications at 140 keV for the 3 collimators are listed in Table 2: 2.8, 5.46, and 8.38 counts/min/kBq for the LEUHR, LEHR, and medium-energy collimator, respectively. The values in Table 3 differ from these because of the addition of the high-energy photons. The sensitivity of a parallel-hole collimator should not change with distance. However, the sensitivity of the low-energy collimators decreases with distance since the high-energy component that is counted because of septal penetration is reduced by the inverse square law. There is essentially no collimation of this high-energy component. On the other hand, the thicker septa of the medium-energy collimator reduce much of the septal penetration by the high-energy photons. Therefore, the sensitivity is nearly unchanged on the medium-energy collimator at the 2 distances. In other words, the counting rate does not change with distance if there is adequate septal thickness (eliminating penetration), but the counting rate decreases with distance if the septal thickness is not adequate. The sensitivity of the medium-energy collimator is about 55% higher than that of the LEUHR collimator and is also higher than the commonly used LEHR collimator (Table 2).

The results of the Jaszczak phantom experiments are shown in Figure 2. Looking at the planar image using the LEUHR or LEHR collimator, one can see a substantial number of counts outside the boundaries of the phantom that are due to septal penetration of the higher-energy photons. These photons lead to increased background activity in the image that reduce contrast, making the features in the image (in this case the hot rods) more difficult to discern. The rods in the fifth sector (those located at 5 o'clock) can be discerned in the medium-energy image on the right but cannot be distinguished in the LEUHR or LEHR images. The contrast of the largest rods is also substantially better with the medium-energy collimator than with the LEUHR and LEHR collimators. Not only is the contrast better with the medium-energy collimator, but the image appears to be less noisy even though all 3 images were acquired for the same number of total counts. In the medium-energy case, most of the counts are, in fact, within the object of interest, whereas with the LEUHR and LEHR collimators many of the counts are actually outside the object. Thus, the quality of the medium-energy image is substantially better than that of the LEUHR and LEHR images.

TABLE 3
System Sensitivity (in Counts per Minute per Kilobecquerel) of ^{123}I Versus Distance for LEUHR, LEHR, and Medium-Energy Collimators

Distance (cm)	LEUHR	LEHR	Medium-energy
0	6.59	14.32	8.00
10	5.51	12.30	7.97

Comparing the SPECT images, the contrast of the cold spheres appears to be slightly improved with the medium-energy collimator. However, there are more counts that appear outside the object in the form of streaks for the LEUHR image than for the medium-energy image. Therefore, the improved sensitivity of the medium-energy collimator and the fact that more of the counts are within the object lead to a notable improvement in image quality for the medium-energy SPECT images as well.

Figures 3 and 4 show clinical examples using the 2 collimators. The medium-energy images were acquired several months after the LEUHR images, and thus the biodistribution is most likely different on the 2 dates. Figure 3 is a ^{123}I-MIBG study of a 7-y-old with stage 4 neuroblastoma. As with the phantom experiment, the image quality is substantially better using the medium-energy collimator than using the LEUHR collimator because of the improved contrast and noise reduction. Figure 4 is a ^{123}I-NaI study of a 17-y-old with thyroid cancer. Again the image quality is clearly improved with the medium-energy collimator relative to the LEUHR collimator.

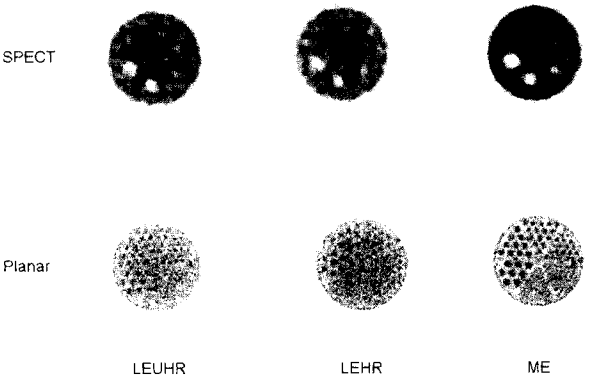

FIGURE 2. This figure shows SPECT and planar images acquired with a tomographic phantom filled with ^{123}I. The phantom was imaged with LEUHR, LEHR, and medium-energy (ME) collimators. On the images using low-energy collimators, many events are localized outside the boundary of the phantom because of septal penetration. Image quality is better for the medium-energy-collimator images than for low-energy-collimator images because of higher contrast and lower noise.

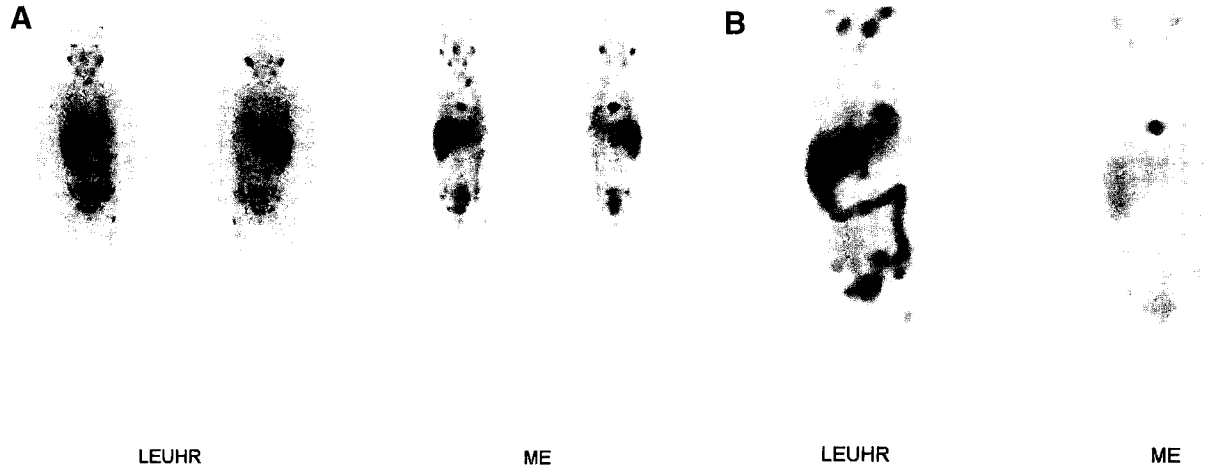

FIGURE 3. Whole-body planar (A) and SPECT (B) images of ^{123}I-MIBG study in a 7-y-old patient with stage 4 neuroblastoma. Images on left were acquired during initial visit when we were using LEUHR collimators, and those on right were acquired several months later when we had modified our acquisition protocol to use medium-energy (ME) collimators. SPECT images are anterior maximum-intensity-projection images. Results are similar to the phantom results. For both whole-body planar imaging and SPECT, images obtained using medium-energy collimators demonstrated less septal penetration (fewer counts outside patient), higher contrast, and less noise.

DISCUSSION

Our results clearly show the improvement in image quality for both planar imaging and SPECT when a medium-energy collimator is used instead of a low-energy collimator for the imaging of ^{123}I-labeled radiopharmaceuticals, including ^{123}I-MIBG. This improvement is due to the substantial reduction of septal penetration of the high-energy (greater than 400 keV) γ-rays emitted by ^{123}I. Although the primary γ-ray associated with ^{123}I has an energy of 159 keV, which is well suited for imaging with low-energy collimators, almost 3% of the photons emitted by ^{123}I have energies above 400 keV. The interhole septa of the low-energy collimator are not effective at stopping these high-energy γ-rays, and thus it is estimated that almost half the photons detected in the 159-keV energy window of the γ-camera actually result from these high-energy photons (*5*). The collimators investigated in this article were from a single manufacturer, and the characteristics and performance of medium-energy and low-energy collimators from another manufacturer may vary with respect to ^{123}I.

The images in Figure 2 that were acquired with the LEUHR and LEHR collimators show a substantial number of events occurring outside the boundaries of the phantom that are the result of septal penetration of high-energy photons. Figure 2 demonstrates that this is true for both planar imaging and SPECT. The presence of this septal penetration leads to a loss of image contrast and thereby image quality. This degradation in image quality can compromise the diagnostic accuracy of the clinical ^{123}I studies, including ^{123}I-MIBG and ^{123}I-NaI, and make it more difficult to discern changes between the current and previous studies on the same patient.

The medium-energy collimator has thicker septa than the low-energy collimators and thereby is more effective in reducing the septal penetration of the high-energy photons. de Vries et al. applied Monte Carlo simulation to show that the use of a medium-energy collimator could reduce the septal penetration of 320-keV photons by a factor of more than 2 (*10*). Table 2 compares the collimators used in this investigation, and the calculations indicate that the medium-energy collimator reduces septal penetration relative to the LEUHR and LEHR collimators from greater than 40% to 4.9% for 300-keV photons and greater than 70% to 30% for 500-keV photons. The effect of reduction of septal penetration on image quality, both planar and SPECT, is clearly seen in Figure 2. The events outside the boundaries of the object are substantially reduced in the medium-energy relative to the LEUHR images. Again, this reduction

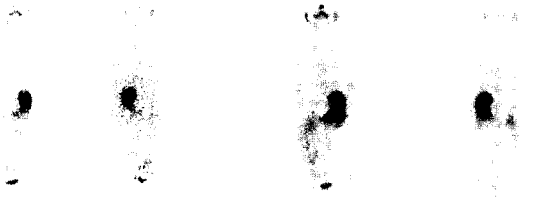

FIGURE 4. Whole-body planar images of ^{123}I-NaI study in a 17-y-old patient being evaluated for thyroid cancer. Images on left were acquired during initial visit when we were using LEUHR collimator, and those on right were acquired several months later when we had modified our acquisition protocol to use medium-energy (ME) collimator. Results are similar to the phantom results. Images obtained using medium-energy collimator demonstrated less septal penetration (fewer counts outside patient), higher contrast, and less noise.

in septal penetration leads to an improvement in image contrast and, thereby, in image quality. In fact, the reduction in septal penetration and improvement in contrast outweigh the loss of spatial resolution, leading to an overall improvement in image quality.

This improvement in image quality is also demonstrated in the clinical examples shown in Figures 3 and 4. In both these cases, the initial scan was acquired using the LEUHR collimator as was defined by our imaging protocol at the time. Not long after these initial scans, the phantom experiments described in this article were performed, and on the basis of these results, our protocol was modified for the use of the medium-energy collimator. In Figure 3, the results of the ^{123}I-MIBG patient are shown for both whole-body planar imaging and SPECT. When these 2 patients returned for their follow-up scan a few months later, they were imaged with the medium-energy collimator. Because in both cases the images were acquired several months apart, the distribution of the radiopharmaceutical could have changed. However, the improvement in image quality between the techniques is clearly demonstrated. As shown in Table 3, the extrinsic sensitivity of the medium-energy collimator is substantially higher than that of the LEUHR collimator (8.7 vs. 5.62 counts/min/kBq), with a larger proportion of good events rather than septal penetration events. Thus, from a practical point of view, the medium-energy collimator can acquire images of improved quality within a shorter time.

CONCLUSION

We have shown that the use of medium-energy collimators leads to improved image quality relative to low-energy collimators for imaging ^{123}I-labeled radiopharmaceuticals, including ^{123}I-MIBG for patients with neuroblastoma and ^{123}I-NaI for patients with metastatic thyroid cancer. This improvement in image quality is due to a reduction in the septal penetration of high-energy γ-rays, which are emitted by ^{123}I in low abundance. In our clinic, we have modified our ^{123}I image protocols to use a medium-energy collimator, leading to a notable improvement in our clinical images.

REFERENCES

1. *ICRP Publication 53: Radiation Dose to Patients from Radiopharmaceuticals: International Commission on Radiological Protection*. London, U.K.: Pergamon Press; 1987.
2. *ICRP Publication 80: Radiation Dose to Patients from Radiopharmaceuticals. International Commission on Radiation Protection*. London, U.K.: Pergamon Press; 1997.
3. Vik TA, Pfluger T, Kadota R, et al. ^{123}I-mIBG scintigraphy in patients with known or suspected neuroblastoma: results from a prospective multicenter trial. *Pediatr Blood Cancer.* 2009;52:784–790.
4. *ICRP Publication 38: Radionuclide Transformation—Energy and Intensity of Emissions*. London, U.K.: Pergamon Press; 1983.
5. Cot A, Sempau J, Pareto D, et al. Study of the point spread function (PSF) for ^{123}I SPECT imaging using Monte Carlo simulation. *Phys Med Biol.* 2004;49:3125–3136.
6. Dobbeleir AA, Hambye ASE, Franken PR. Influence of high-energy photons on the spectrum of iodine-123 with low- and medium-energy collimators: consequences for imaging with ^{123}I-labelled compounds in clinical practice. *Eur J Nucl Med.* 1999;26:655–658.
7. Chen J, Garcia EV, Galt JR, et al. Improved quantification in ^{123}I cardiac SPECT imaging with deconvolution of septal penetration. *Nucl Med Commun.* 2006;27:551–558.
8. Verberne HJ, Feenstra C, de Jong WM, et al. *Eur J Nucl Med Mol Imaging.* 2005; 32:1100–1107.
9. NEMA Standards Publication NU 1-2007. Performance Measurements of Gamma Cameras.
10. de Vries DJ, Moore SC, Zimmerman RE, et al. Development and validation of a Mone Carlo simulation of photon transport in an Anger camera. *IEEE Trans Med Imaging.* 1990;9:430–438.